

THE COMPOSITION RANGE AND  
CRYSTAL STRUCTURE OF  $\text{Ti}_2\text{Ni}$

GEORGE ALLEN YURKO

For Reference

NOT TO BE TAKEN FROM THIS ROOM

Thesis  
1959  
#38

Ex LIBRIS  
UNIVERSITATIS  
ALBERTAENSIS







Digitized by the Internet Archive  
in 2018 with funding from  
University of Alberta Libraries

<https://archive.org/details/yurko1959>

11515  
1959  
#38

THE UNIVERSITY OF ALBERTA

THE COMPOSITION RANGE AND CRYSTAL STRUCTURE OF  $Ti_2Ni$

A DISSERTATION

SUBMITTED TO THE FACULTY OF GRADUATE STUDIES  
IN PARTIAL FULFILMENT OF THE REQUIREMENTS FOR THE DEGREE  
OF MASTER OF SCIENCE

DEPARTMENT OF MINING AND METALLURGY

by

GEORGE ALLEN YURKO

EDMONTON, ALBERTA

APRIL, 1959



## ABSTRACT

The composition range and crystal structure of  $\text{Ti}_2\text{Ni}$  were investigated. Homogeneous high purity alloys were prepared from iodide titanium and spectrographic standard nickel by levitation melting.

X-ray diffraction and optical metallographic techniques were used to determine the composition range of  $\text{Ti}_2\text{Ni}$ . X-ray diffraction plots on powder specimens showed the lattice parameter to be the same on both sides of stoichiometric composition. Therefore, if Vegard's law is assumed, a range of composition of not more than 2 pct is indicated. The lattice parameter for  $\text{Ti}_2\text{Ni}$  is  $11.278 \pm .001 \text{ \AA}$ . Microscopical metallography shows that at  $700^\circ\text{C}$  the composition limits lie between 0.5 and 1 pct on either side of stoichiometric composition. At  $900^\circ\text{C}$ , and on slow cooling from  $700^\circ\text{C}$ , the composition limits are less than 0.5 pct on either side of stoichiometric composition. The maximum limits of composition lie between  $700^\circ$  and  $900^\circ\text{C}$  — at  $765^\circ\text{C}$  on the low nickel content side and between  $800^\circ$  and  $900^\circ\text{C}$  on the high nickel content side.

The crystal structure of  $\text{Ti}_2\text{Ni}$  has been determined from powder specimens. The unit cell is face-centered cubic with 96 atoms. The space group is  $O_h^7$  -  $\text{Fd}3\text{m}$ . 64 titanium atoms are in positions 48f and 16c, and 32 nickel atoms are in positions 32e. The atomic parameters,  $X_{\text{Ni}} = 0.215 \pm .001$  and  $X_{\text{Ti}} = 0.810 \pm .002$  were determined







by trial and error. The interatomic distances have been calculated and are discussed. A model of the structure cell has been made.



## ACKNOWLEDGMENTS

The author wishes to thank Dr. J. Gordon Parr under whose capable direction the research in this thesis was performed and E. O. Lilge, Head of the Department of Mining and Metallurgy, for his encouragement. Many stimulating discussions held with staff members J. W. Barton, Dr. R. Taggart, Dr. B. Youdelis and Dr. J. Leja are gratefully acknowledged. Special thanks go to R. M. Scott for his able assistance in preparing specimens for metallographic studies.

Finally, the author wishes to acknowledge with gratitude the funds provided by the Defence Research Board of Canada (7510-27), and the International Nickel Co. of Canada, Ltd.



# TABLE OF CONTENTS

	<u>Page</u>
INTRODUCTION . . . . .	1
PART I - THE COMPOSITION RANGE OF $Ti_2Ni$ .	
GENERAL . . . . .	2
EXPERIMENTAL TECHNIQUES . . . . .	5
EXPERIMENTAL RESULTS. . . . .	8
DISCUSSION. . . . .	8
PART II - THE CRYSTAL STRUCTURE OF $Ti_2Ni$ .	
GENERAL . . . . .	19
EXPERIMENTAL TECHNIQUES . . . . .	21
EXPERIMENTAL RESULTS. . . . .	21
DETERMINATION OF STRUCTURE	
Introduction . . . . .	24
Preliminary Investigations . . . . .	28
Calculation of Structure . . . . .	33
DISCUSSION OF STRUCTURE . . . . .	39
SUMMARY OF RESULTS AND CONCLUSIONS . . . . .	45
BIBLIOGRAPHY . . . . .	47
APPENDIX I - LEVITATION MELTING. . . . .	48
APPENDIX II - GAS QUENCHING . . . . .	51



# TABLES

	<u>Page</u>
I. Analysis of Iodide Titanium . . . . .	6
II. Analysis of Spectrographic Standard Nickel . . . . .	6
III. Lattice Parameter of $Ti_2Ni$ . . . . .	9
IV. Summary of Metallographic Results . . . . .	10
V. Summary of X-ray Diffraction Data of $Ti_2Ni$ Recorded by Duwez and Taylor. . . . .	20
VI. Comparison of Calculated and Observed Intensities in Nickel. . . . .	27
VII. Arrangement of Atoms in the Multiple Face-Centered Cubic Cell . . . . .	30
VIII. $O_h^7$ - $Fd3m$ Space Group - International Tables. . . . .	32
IX. Comparison of Observed and Calculated Intensities in $Ti_2Ni$ . . . . .	36
X. Coordinates of Titanium and Nickel Atoms . . . . .	38
XI. Interatomic Distances in $Ti_2Ni$ . . . . .	43





# ILLUSTRATIONS

	<u>Page</u>
1. Constitutional diagram of the titanium-nickel system. .	4
2. 33.33 pct Ni. Annealed at 700°C. $Ti_2Ni$ . . . . .	14
3. 32.37 pct Ni. Quenched from 700°C. $Ti_2Ni$ with $\infty$ ppte at grain boundaries. . . . .	14
4. 34.26 pct Ni. Quenched from 700°C. $TiNi$ ppte in $Ti_2Ni$ matrix. . . . .	15
5. 32.87 pct Ni. Annealed at 700°C. $Ti_2Ni$ with $\infty$ ppte at grain boundaries . . . . .	15
6. 33.71 pct Ni. Annealed at 700°C. $Ti_2Ni$ with $TiNi$ ppte at grain boundaries . . . . .	16
7. 32.87 pct Ni. Quenched from 900°C. $Ti_2Ni$ with $\beta$ ppte at grain boundaries . . . . .	16
8. 33.71 pct Ni. Quenched from 900°C. $Ti_2Ni$ with $TiNi$ ppte at grain boundaries . . . . .	17
9. Section of constitutional diagram showing the range of composition of $Ti_2Ni$ . . . . .	18
10. Powder photograph of $Ti_2Ni$ reflections. . . . .	23
11. Structure of diamond. . . . .	29
12. Section of multiple face-centered cubic cell. . . . .	29
13. Change in ratio of calculated structure factors with nickel parameter. . . . .	34
14. Change in ratio of calculated structure factors with titanium parameter. . . . .	35
15. Model of $Ti_2Ni$ structure cell . . . . .	40
16. Representative portion of cell. . . . .	41
APPENDIX I 1. Levitation melting unit. . . . .	49
2. Levitation melting unit in operation . . . . .	49
APPENDIX II 1. Gas quenching unit for powder specimens. . .	52



## INTRODUCTION

The purpose of this investigation is an attempt to obtain the complete crystal structure and composition limits of the phase  $\text{Ti}_2\text{Ni}$ . Since titanium is a highly reactive element, all possible precautions against contamination were taken.

To facilitate presentation of results, the work will be discussed under two headings:

- (1) The Composition Range of  $\text{Ti}_2\text{Ni}$ , and
- (2) The Crystal Structure of  $\text{Ti}_2\text{Ni}$ .



## PART I

### THE COMPOSITION RANGE OF $Ti_2Ni$





## THE COMPOSITION RANGE OF $Ti_2Ni$

### GENERAL

The titanium - nickel system (30 - 100 pct <sup>\*</sup>Ni) was first studied in Germany by Wallbaum and his associates<sup>1,2</sup> in the period 1937 - 1942. The alloys used, however, were prepared from low purity titanium (95 pct) and were melted in refractory crucibles under an argon atmosphere. Since titanium is a highly reactive element, the technique used for alloy preparation resulted in contamination. Reaction occurred with the crucible and, in thermal analysis work, with the thermocouple sheath. The results, therefore, though they provide a general picture of the nickel-rich region of the system, may not be accurate in detail.  $Ti_2Ni$  was stated to be complex face-centered cubic with 96 atoms per cell.

Further work on the system was later carried out by Long<sup>3</sup> and by McQuillan<sup>4</sup>. The results of Long were not reliable because of the lack of purity of titanium. McQuillan used higher purity titanium (magnesium - reduced titanium, commonly known as sponge titanium - 99.5 pct purity) in determining the position of the  $\alpha / (\alpha + \beta)$  boundary in alloys containing up to 4 pct Ni.

\* pct refers to Atomic percent throughout the thesis unless otherwise specified.



The most extensive study of the system so far published is that of Margolin et al<sup>5</sup>, whose work was based on arc-melted alloys prepared from both iodide titanium and sponge titanium, and covered the composition range to about 65 pct nickel. The diagram presented in Figure 1 is based largely on the results of this investigation. The  $\text{Ti}_2\text{Ni}$  phase is represented by a straight line, which implies that there is no range of composition.

Duwez and Taylor<sup>6</sup> concentrated their investigations on the  $\text{Ti}_2\text{Ni}$  and  $\text{TiNi}$  region. The alloys were prepared by sintering powdered sponge titanium and nickel for 4 hours @  $925^\circ\text{C}$  in a vacuum of  $10^{-4}$  mm. of mercury. Results showed  $\text{Ti}_2\text{Ni}$  as face-centered cubic with a lattice parameter of 11.310 kx units, but no composition range was indicated. Investigations of the body-centered cubic  $\text{TiNi}$  phase showed that after prolonged heating at  $800^\circ\text{C}$  this phase decomposed to a eutectoid of  $\text{Ti}_2\text{Ni}$  and  $\text{TiNi}_3$  upon cooling. There is no indication of this in the constitutional diagram proposed by Margolin et al. Rostoker and his associates,<sup>7,8</sup> using iodide titanium and arc-melting techniques for the preparation of  $\text{Ti}_2\text{Ni}$ , obtained a lattice parameter of  $11.29 \text{ \AA}$  and found the composition range to be narrow but no precise limits were given.

The purpose of this investigation was to prepare homogeneous



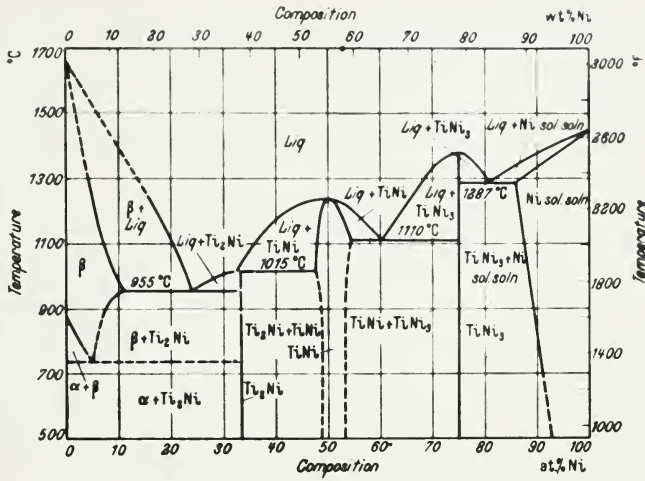


Figure 1. Constitutional diagram of the titanium-nickel system.



alloys on either side of the stoichiometric composition (33.33 pct Ni) and to determine by metallographic techniques — both optical and X-ray diffraction — the composition limits of the phase.

#### EXPERIMENTAL TECHNIQUES

Alloys of iodide titanium (99.9 + pct) and spectrographic standard nickel (99.99 + pct) were prepared by levitation melting in an inert atmosphere of argon (Appendix I). Analysis of the impurities in iodide titanium and spectrographic standard nickel are recorded in Table 1 and 2 respectively. Weighing the components before and after melting determined that any error of composition was very small and never exceeded 0.03 pct by weight. Homogeneity of the alloys was investigated by taking powder samples of several alloys and examining them metallographically. Identical microstructures were observed for all particles of each sample. Therefore homogeneity was assumed in all alloys after levitating and casting.

A series of alloys containing from 20 to 45 pct Ni (Table III) was prepared for X-ray diffraction in the following manner: Crushed particles (-200 mesh) from each alloy were annealed at 700°C for 15 minutes in a molybdenum boat within a sealed evacuated silica capsule. Crushed particles of several of these alloys were also quenched from that temperature by argon





Table I - Analysis of Iodide Titanium

<u>Element</u>	<u>Amount-pct</u>
Si	0.004
Al	0.003
Mg	0.005
Mn	0.008
Fe	0.002
Cr	Trace
Ni	Trace
Sn	0.006
Cu	0.002
Ca	0.008
Mo	N.D.
Zr	less than 0.05

Table II - Analysis of Spectrographic Standard Nickel

<u>Element</u>	<u>Estimate of Quantity Present</u> <u>parts per million</u>
Fe	8
Si	6
Al }	2
Ca }	
Cu }	1
Na }	
Mg }	each less than 1
Ag }	

Elements specifically sought but not detected:

As, Au, B, Ba, Be, Bi, Cd, Co, Cr, Cs, Ga, Ge, Hf, Hg, In,  
Ir, K, Li, Mn, Mo, Nb, Os, P, Pb, Pd, Pt, Rb, Re, Rh, Ru,  
Sb, Se, Sn, Sr, Ta, Te, Ti, Tl, V, W, Zn, Zr.



gas (Appendix II). Microhardness tests on pure titanium particles showed no measurable contamination due to these treatments.

X-ray diffraction plots were made on the powders (using Geiger spectrometer and  $\text{Co K}\alpha$  radiation) on the assumption that if a composition range existed,  $\text{Ti}_2\text{Ni}$  would show one value of lattice parameter in the two-phase field  $\alpha + \text{Ti}_2\text{Ni}$ , and a different parameter in the two-phase field  $\text{TiNi} + \text{Ti}_2\text{Ni}$ . That is, alloys containing 20, 25 and 30 pct Ni would show one parameter value, while the alloys containing 35, 40 and 45 pct Ni would show a different value. If these two parameter values differed then approximate composition limits could be established by obtaining parameter values of the alloys near the stoichiometric composition.

Fairly accurate parameter measurements were obtained by mixing pure nickel powder with each sample, and plotting intensities of both nickel reflections and selected  $\text{Ti}_2\text{Ni}$  reflections at intervals of 0.005 deg. Bragg angle. The nickel reflections were, of course, used as a standard; and the plots established accurate reflection peaks.

A series of alloys was next prepared whose compositions (nickel content) were: 33.33, 32.37, 32.87, 33.71, and 34.26 pct. Crushed particles were annealed and quenched, as



before, and examined metallographically. Soaking temperatures were 700° and 900°C.

#### EXPERIMENTAL RESULTS

The lattice parameters obtained for alloys whose compositions ranged from 20 to 45 pct Ni are summarized in Table III. It will be observed that no difference in parameter is detected in the alloys containing more than or less than stoichiometric composition. This will be discussed later.

Metallographic results are summarized in Table IV, which makes reference to pertinent photomicrographs.

#### DISCUSSION OF RESULTS

Within the limits of accuracy of the method, X-ray diffraction results show that the lattice parameter of  $\text{Ti}_2\text{Ni}$  is the same on both sides of the stoichiometric composition. The mean value for the lattice parameter of  $\text{Ti}_2\text{Ni}$  is  $11.278 \pm .001$  Ångströms. This value compares with values quoted by Hansen, McPherson, and Rostoker<sup>7</sup> of  $11.29$  Å. A lower lattice parameter value probably indicates that the technique used for alloy preparation resulted in less contamination or that the method used for determining reflection peaks was more accurate.





Table III - Lattice Parameter of  $\text{Ti}_2\text{Ni}$  ( $\text{\AA}$  Units)

<u>Lattice Parameter</u>				
<u>Pct Ni</u>	<u>Using Line 333</u>	<u>Using Line 440</u>	<u>Using Line 600</u>	<u>Mean Lattice Parameter</u>
20	11.278	11.279	11.277	11.278
25	11.278	11.279	11.277	11.278
30	11.278	11.275	11.277	11.277
31.50	11.278	11.280	11.277	11.278
32.87	11.278	11.279	11.277	11.278
33.33	11.278	11.279	11.280	11.279
33.71	11.278	11.279	11.277	11.278
35	11.278	11.279	11.280	11.279
40	11.278	11.280	11.277	11.278
45	11.278	11.279	11.277	11.278



Table IV - Summary of Metallographic Results

Composition (pct Ni)	Annealed Structure	Quenched Structure	
		700°	900°
33.33	Single-phase (Figure 2)	Single-phase (As Figure 2)	Single-phase (As Figure 2)
32.87	Two-phase (Figure 5)	Single-phase (As Figure 2)	Two-phase (Figure 7)
32.37	Two-phase	Two-phase (Figure 3)	Two-phase
33.71	Two-phase (Figure 6)	Single-phase (As Figure 1)	Two-phase (Figure 8)
34.26	Two-phase	Two-Phase (Figure 4)	Two-phase



Approximate calculations using atomic radii of titanium and nickel and applying Vegard's law, show that a range of composition of  $Ti_2Ni$  of not less than 2 pct Ni must exist if any lattice parameter change is to be detected within the limits of accuracy of the method described. Consequently, it is reasonable to conclude that the composition range of  $Ti_2Ni$  at  $700^{\circ}C$  is less than 2 pct Ni. Further, since precipitation of a second phase would be expected on slow cooling through a phase boundary, the results also imply that at temperatures below  $700^{\circ}C$  the composition range does not exceed 2 pct Ni.

Microstructures of annealed and quenched alloys (33.33, 32.87, 32.37, 33.71 and 34.26 pct Ni) are shown in Figures 2 to 8. The single phase of stoichiometric  $Ti_2Ni$  is shown in Figure 2. Single-phase structures are also produced by quenching from  $700^{\circ}C$  alloys containing 0.5 pct Ni more than or less than stoichiometric composition. Alloys containing 1 pct more than or less than stoichiometric composition show a two-phase structure. Figure 3 shows  $Ti_2Ni$  with  $\alpha$  - titanium precipitated at the grain boundaries after quenching. Figure 4 shows  $TiNi$  phase precipitated in the  $Ti_2Ni$  matrix. It is therefore concluded that at  $700^{\circ}C$ , the composition limits for  $Ti_2Ni$  lie between 0.5 and 1 pct on either side of stoichiometric



composition.

Annealed alloys containing 0.5 pct Ni more than or less than stoichiometric composition show two-phase structures, indicating that the composition range of  $\text{Ti}_2\text{Ni}$  narrows as the temperature decreases from  $700^\circ\text{C}$ . Figure 5 shows  $\text{Ti}_2\text{Ni}$  with  $\alpha$  - titanium precipitated at the grain boundaries after annealing. Figure 6 shows  $\text{TiNi}$  precipitating at the  $\text{Ti}_2\text{Ni}$  grain boundaries.

Alloys quenched from  $900^\circ\text{C}$  containing 0.5 pct Ni more than or less than stoichiometric composition show a two-phase structure as indicated by Figures 7 and 8. Figure 7 shows  $\text{Ti}_2\text{Ni}$  with  $\beta$  - titanium precipitated at the grain boundaries. Figure 8 shows  $\text{Ti}_2\text{Ni}$  with  $\text{TiNi}$  precipitated at the grain boundaries. Since the composition limits at  $900^\circ$  are less than those at  $700^\circ\text{C}$ , it appears that as the temperature increases above  $900^\circ\text{C}$  the composition limits decrease and come to a point at the peritectic temperature ( $1015^\circ\text{C}$ ).

The extreme composition limits of  $\text{Ti}_2\text{Ni}$  lie between  $700^\circ$  and  $900^\circ\text{C}$ . Since the transformation of  $\beta$  - titanium to  $\alpha$  - titanium occurs at the eutectoid temperature of  $765^\circ\text{C}$ , the minimum nickel content of  $\text{Ti}_2\text{Ni}$  would be expected to occur at this temperature, since a change in the slope of the solubility





line may occur only at a phase transformation. The maximum nickel content of  $\text{Ti}_2\text{Ni}$  occurs between  $700^\circ$  and  $900^\circ\text{C}$ . The constitutional diagram (Figure 1) proposed by Margolin et al<sup>5</sup> indicates no transformation within this temperature range on the nickel-rich side. However, Duwez and Taylor's<sup>6</sup> investigations showed that the  $\text{TiNi}$  phase is unstable. From their cursory experiment they concluded that  $\text{TiNi}$  decomposes into  $\text{Ti}_2\text{Ni}$  and  $\text{TiNi}_3$  upon cooling from a temperature of  $800^\circ\text{C}$  or above. While the evidence strongly indicates a transformation, the actual temperature of the transformation cannot be unequivocally stated. However, it probably lies between  $900^\circ$  and  $800^\circ\text{C}$ , and would probably be reported by a eutectoid horizontal joining the solubility lines of  $\text{Ti}_2\text{Ni}$  and  $\text{TiNi}_3$ . Such a construction on a constitutional diagram is consistent with the observations recorded in the present work. That is, the slope of the solubility line on the nickel-rich side of  $\text{Ti}_2\text{Ni}$  changes between  $700^\circ$  and  $900^\circ\text{C}$ .

A portion of the titanium-nickel constitutional diagram indicating the range of composition of  $\text{Ti}_2\text{Ni}$  is shown in Figure 9.



# MICROSTRUCTURES

All specimens etched in 4 pct HF in water, rinsed in 4 pct  $\text{HNO}_3$ .  
All photomicrographs at 400x magnification.

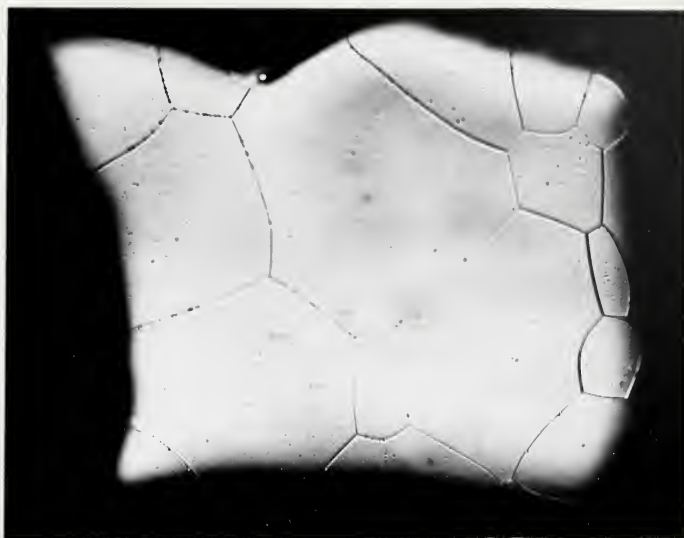


Figure 2. 33.33 pct Ni. Annealed at 700°C.  $\text{Ti}_2\text{Ni}$ .

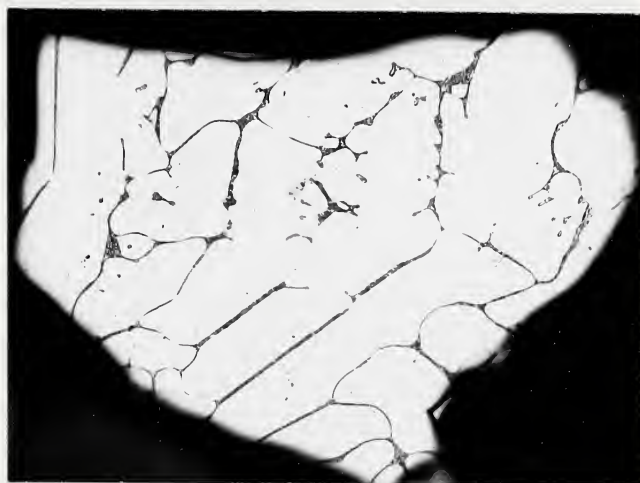


Figure 3. 32.37 pct Ni. Quenched from 700°C.  
 $\text{Ti}_2\text{Ni}$  with  $\alpha$ -ppte at grain boundaries.



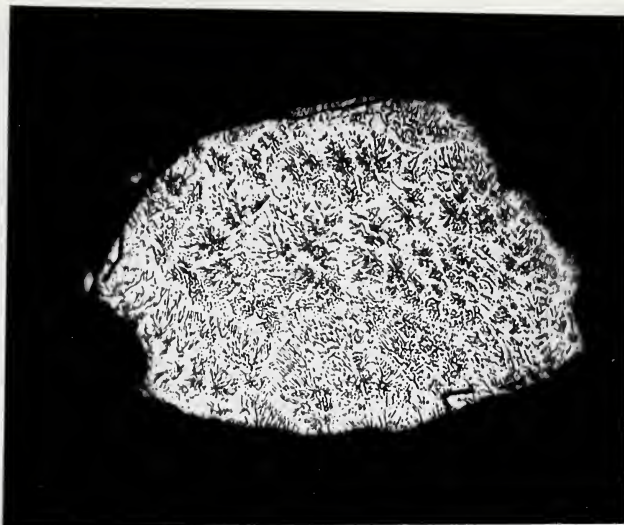


Figure 4. 34.26 pct Ni. Quenched from 700°C.  
TiNi ppte in  $Ti_2Ni$  matrix.

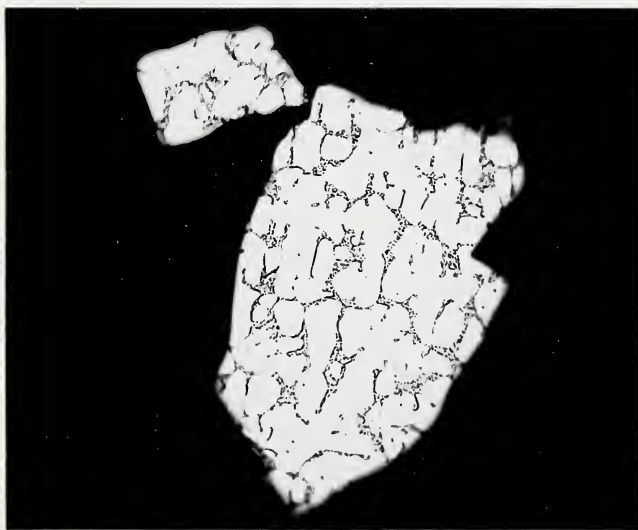


Figure 5. 32.87 pct Ni. Annealed at 700°C.  
 $Ti_2Ni$  with  $\alpha$  ppte at grain boundaries.



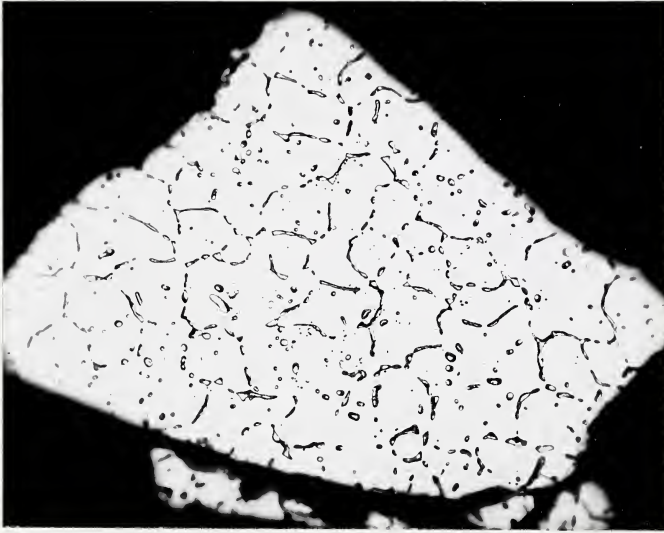


Figure 8. 33.71 pct Ni. Quenched from 900°C.  
 $\text{Ti}_2\text{Ni}$  with  $\text{TiNi}$  ppte at grain boundaries.





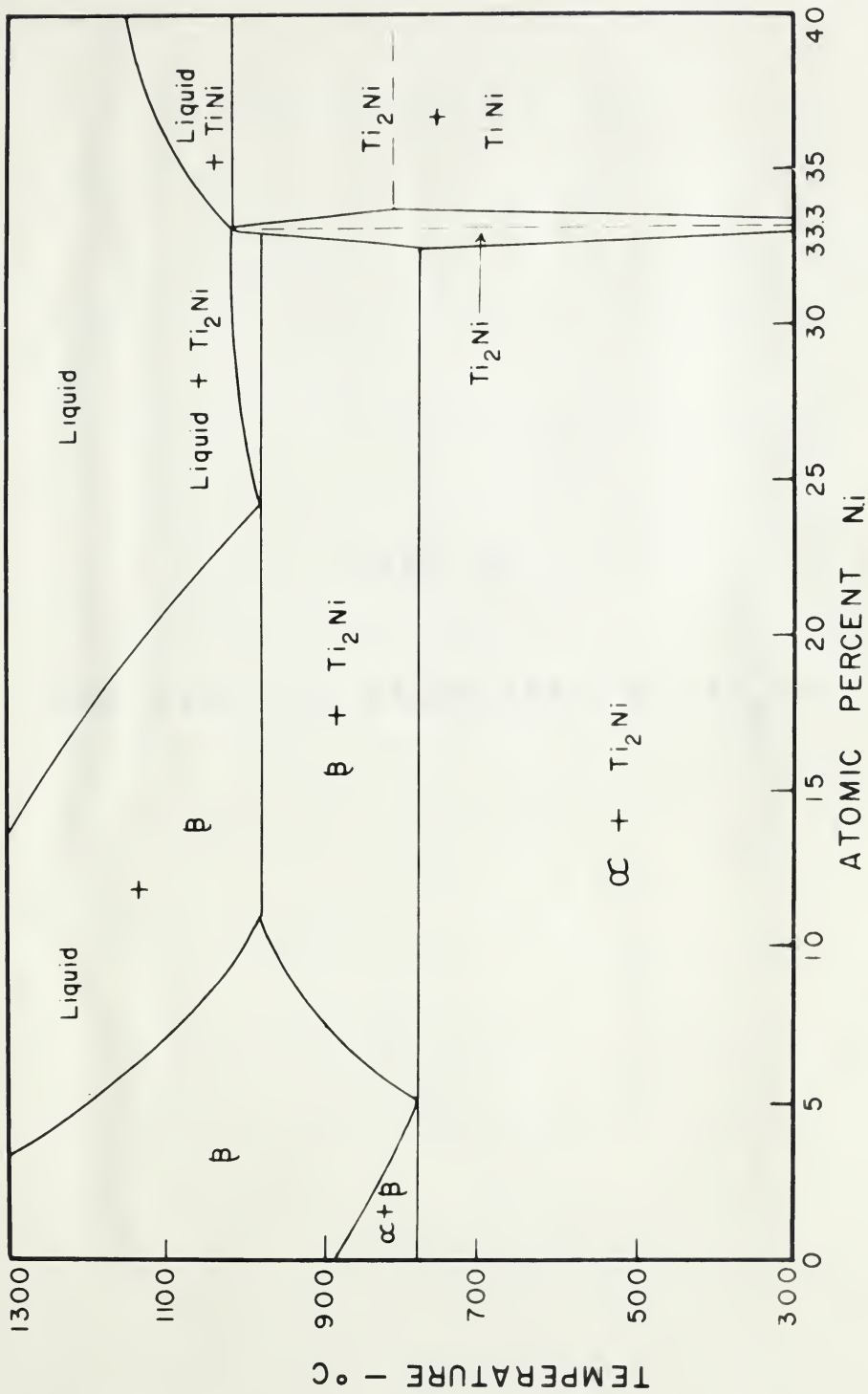


Figure 9. Section of constitutional diagram showing the range of composition of Ti<sub>2</sub>Ni.



PART II

THE CRYSTAL STRUCTURE OF  $\text{Ti}_2\text{Ni}$



## THE CRYSTAL STRUCTURE OF $\text{Ti}_2\text{Ni}$

### GENERAL

Laves and Wallbaum<sup>1</sup> described the structure of  $\text{Ti}_2\text{Ni}$  as complex face-centered cubic with 96 atoms per unit cell. No value of cell constant was given.

Duwez and Taylor<sup>6</sup> investigated several  $\text{Ti}_2\text{X}$  phases and found  $\text{Ti}_2\text{Ni}$  to be face-centered cubic, with a density of  $5.77 \text{ g. cm}^{-3}$  and lattice parameter of 11.310 kx units from which the number of molecules per cell was computed to be approximately 32 (96 atoms). (However, calculations from the data show that there are 98 atoms per unit cell — therefore the number of molecules could be 33 and not 32.) Duwez and Taylor's X-ray diffraction studies on powders were carried out with a 14.32 cm diameter camera, using  $\text{Co K}\alpha$  radiation. Their results are summarized in Table V.

Rostoker<sup>8</sup> reported the structure of  $\text{Ti}_2\text{Ni}$  to be face-centered cubic ( $\text{Fe}_3\text{W}_3\text{C}$  type) and the cell constant to be  $11.29 \text{ \AA}$ .

The purpose of the investigation described in this thesis was to obtain the complete crystal structure of the phase.



Table V - Summary of X-ray Diffraction Data of  $Ti_2Ni$

Recorded by Duwez and Taylor<sup>6</sup>

hkl	Interplanar Spacing (kx)*	hkl	Interplanar Spacing (kx)*
111	6.53 w	951-773	1.095 vw
220	3.97 vw	666	1.087 vw
222	3.26 w	775	1.019 vw
400	2.83 vw	955-971	0.9886 w
331	2.59 w	882	0.9847 w
422	2.31 m	866	0.9697 w
333-511	2.17 s	10,62	0.9563 vw
440	2.00 m	12,00-884	0.9423 m
531	1.91 vw	11,51-777	0.9330 m
442-600	1.88 w	12,22-10,64	0.9172 m
622	1.72 w	11,53-975	0.9090 vw
444	1.63 w	12,40	0.8935 vw
551-711	1.59 w	10,82	0.8726 vw
642	1.51 w	13,11-11,55-11,71-993	0.8648 w
553-731	1.472 w	11,73-13,31-977	0.8456 w
800	1.413 vw	13,33-955	0.8277 vw
733	1.382 w	888	0.8162 vw
660-822	1.334 m	13,51-11,75	0.8095 vw
555-751	1.305 w	14,20-10,86	0.7997 w
911-753	1.242 vw	14,22-10,10,2	0.7920 w
842	1.234 w	12,80	0.7842 w
931	1.185 vw		
933-771-755	1.136 m		
862	1.109 vw		

\*The kx unit is defined on the basis of the Siegbahn scale of X-ray wave lengths.  $1\text{\AA} = 1.00202$  kx units.

s = strong

m = medium

w = weak

vw = very weak





## EXPERIMENTAL TECHNIQUES

The preparation of stoichiometric  $\text{Ti}_2\text{Ni}$  has already been described (Part I). In order that the number of atoms per unit cell could be evaluated, a density determination of  $\text{Ti}_2\text{Ni}$  was necessary. Density measurements were made by the displacement method using a 50 ml pycnometer. The density of distilled water at  $20^\circ\text{C}$  was determined and this value was used for  $\text{Ti}_2\text{Ni}$  density calculations. All measurements were made at  $20^\circ\text{C}$ .

Chill-cast ingots of  $\text{Ti}_2\text{Ni}$  were not used for the density determination, since gas cavities are often associated with this type of casting. Hence, the ingots were crushed and a 25 gram sample of -200 mesh particles, annealed for 12 hours at  $700^\circ\text{C}$  was used. Annealing relieved lattice strain produced by crushing.

X-ray diffraction data were obtained on annealed powder specimens by the Geiger spectrometer and the Philips 11.483 cm diameter powder camera, using  $\text{Co K}\alpha$  radiation. Reflections too weak to be measured on the diffractometer charts were obtained by a 48 hour exposure on a powder photograph. A transparent celluloid filter placed before the film reduced the background intensity, thus giving contrasting reflection lines.

## EXPERIMENTAL RESULTS

The measured density of  $\text{Ti}_2\text{Ni}$  at  $20^\circ\text{C}$  was  $5.723 \pm .001 \text{ g. cm}^{-3}$ .

The number of atoms per unit cell is evaluated from the cell



constant and density by the equation:

$$\rho = 1.6602 \frac{\sum A}{V}$$

where:  $\sum A$  is the sum of the atomic weights of the atoms in the unit cell and  $V$  is the volume of the unit cell, in cubic Ångströms.

$$\text{Hence, } 5.723 = 1.6602 \left[ \frac{2/3 \chi (47.90) + 1/3 \chi (58.69)}{(11.278)^3} \right]$$

$$\chi = 96.027$$

That is, the number of atoms in the unit cell = 96.0.

Thirty-seven lines were measured in the powder pattern and were indexed. The lines were found to conform to the face-centered cubic structure. Intensities were obtained by measuring with a planimeter the areas under reflection peaks on two diffractometer charts. Values obtained from the two charts generally agreed to within 5 pct, and an average figure was taken. The intensities of reflections too weak to be measured in this way were visually estimated from the powder photograph, by comparing the weak lines with slightly stronger reflections whose intensities had been measured on the diffractometer chart. The reflection lines obtained on the powder photograph are shown in Figure 10.

The systematic absences were found to obey the following rules:

hkl: absent for hkl mixed odd and even

hhl: absent for  $h + l = 2n + 1$

h00: absent for  $h \neq 4n$

Ok1: absent for  $h \neq 4n$



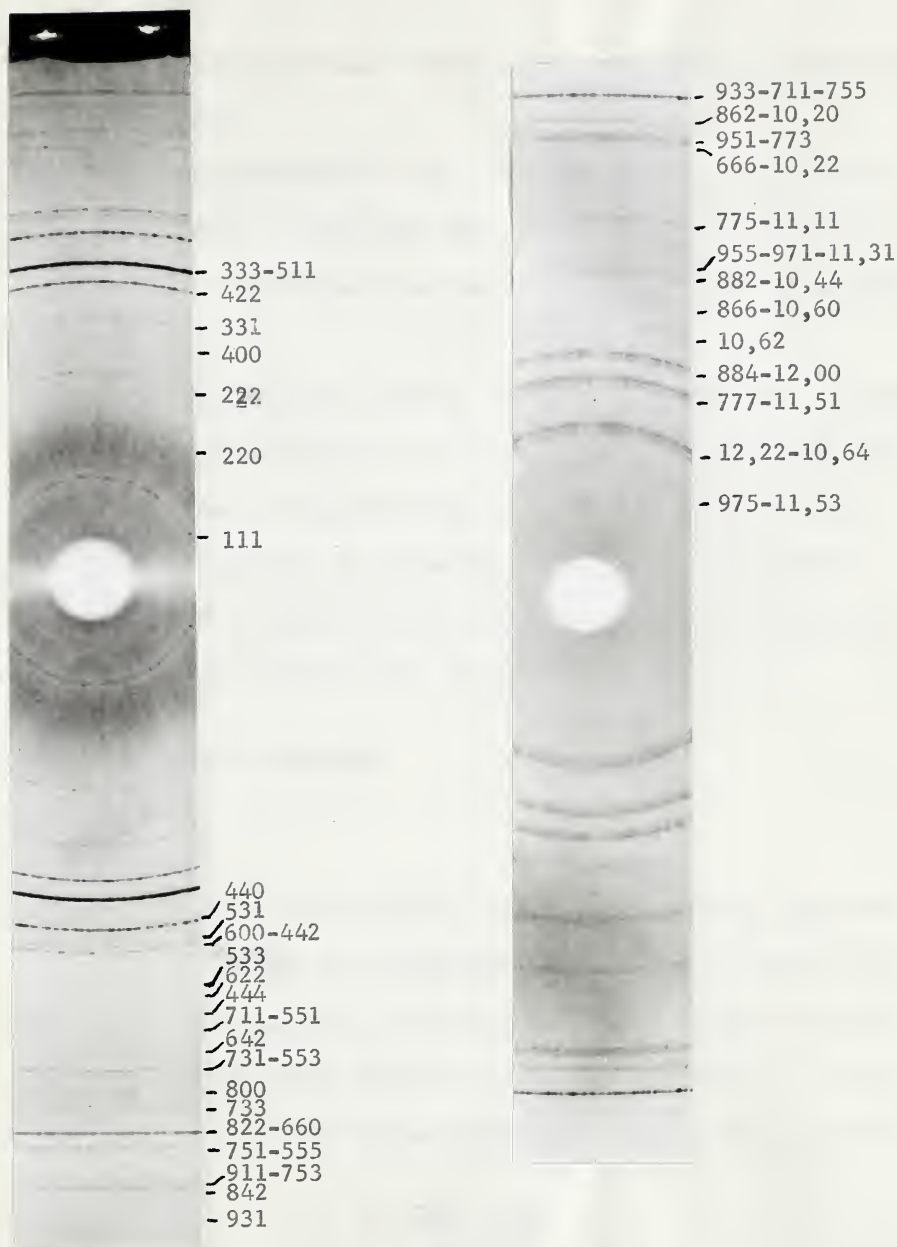


Figure 10. Powder Photograph of  $\text{Ti}_2\text{Ni}$  Reflections.





International tables<sup>9</sup> indicate the most probable space group to be  $O_h^7 - Fd_{3m}$ .

If the reflections for the last two conditions were actually present but were so weak that they could not be seen, then the structure may be obtained from the  $T^2$ ,  $T_d^2$ ,  $T_h^3$ ,  $O^3$ ,  $O^4$  or  $O_h^5$  space group.

The  $O_h^7$  space group contains the face-centered cubic structure and the diamond structure — a structure in which the atoms are arranged on two interpenetrating face-centered cubic lattices. The diamond structure is formed by elements having a ratio of 4 electrons to 1 atom and since titanium is such an element, the  $Ti_2Ni$  structure could be that of diamond.

## DETERMINATION OF STRUCTURE

### Introduction

The structure determination involves calculating reflection line intensities for an arrangement of titanium and nickel atoms. The correct arrangement is obtained when the average discrepancy between calculated and observed intensities is small — usually about 15 percent. The average discrepancy is evaluated from the equation:

$$R = \frac{\sum |I_c - I_o|}{\sum I_o}$$





The intensity of the diffracted beam from a powder is evaluated from the following equation:

$$I = \frac{1 + \cos^2 2\theta}{\sin^2 \theta \cos \theta} \cdot P \cdot /F/^2 \cdot A(\theta) \cdot e^{-\frac{2B \sin^2 \theta}{\lambda^2}}$$

where:  $\frac{1 + \cos^2 2\theta}{\sin^2 \theta \cos \theta}$  is the correction for the Lorentz factor and

the polarization factor.

P is the multiplicity factor — that is, the number of planes corresponding to the form {hkl}.

$/F/^2$  is the structure factor, defined as the ratio of the amplitude of the wave scattered in a given direction by all the atoms in a unit cell to that scattered by a single electron under identical conditions.

$A(\theta)$  is the absorption factor.

$e^{-\frac{2B \sin^2 \theta}{\lambda^2}}$  is the temperature factor.

The absorption and temperature factor corrections are usually small and may be neglected. This will be discussed later.

The structure factor is expressed by the following equation:

$$\begin{aligned} /F/^2 = & \left[ \sum_i f_{Ni} \cos 2\pi (hx + ky + zl) \right]^2 + \left[ \sum_i f_{Ti} \cos 2\pi (hx + ky + zl) \right]^2 \\ & + \left[ \sum_i f_{Ni} \sin 2\pi (hx + ky + zl) \right]^2 + \left[ \sum_i f_{Ti} \sin 2\pi (hx + ky + zl) \right]^2 \end{aligned}$$

where: xyz are the coordinates of the atoms in the unit cell whose



atomic scattering factors are  $f_{Ni}$  and  $f_{Ti}$  for the nickel atoms and the titanium atoms respectively, and where  $hkl$  are the indices of the reflection.

If the structure has a center of symmetry, and the origin of the coordinates is taken at this center of symmetry, then the structure factor equation is reduced to:

$$/F/^2 = \left[ \sum_i f_{Ni} \cos 2\pi(hx + ky + zl) \right]^2 + \left[ \sum_i f_{Ti} \cos 2\pi(hx + ky + zl) \right]^2$$

The scattering factors for nickel and titanium are available in Taylor<sup>10</sup>. The tables for  $\cos 2\pi x$  values are available in Lipson and Cochran<sup>11</sup>.

The effect of omitting absorption and temperature corrections in the intensity calculations was investigated using spectrographic standard nickel. Nickel has a simple face-centered cubic structure with 4 atoms per unit cell and coordinates at 000,  $0\frac{1}{2}\frac{1}{2}$ ,  $\frac{1}{2}0\frac{1}{2}$ , and  $\frac{1}{2}\frac{1}{2}0$ .

The diffractometer chart was obtained (using the procedure described for  $Ti_2Ni$ ) and the reflection peaks 111, 200, 220, 311 and 222 were measured. The structure factor for each reflection was calculated and substituted in the intensity equation:

$$I = \frac{1 + \cos^2 2\theta}{\sin^2 \theta \cos \theta} \cdot P \cdot /F/^2$$

The comparison of the calculated and observed intensities is shown in Table VI. The discrepancy between calculated and observed intensities is small and does not increase with an increase in Bragg



Table VI - Comparison of Observed and Calculated Intensities in Nickel.

hkl	$\theta$	$\frac{1 + \cos^2 2\theta}{\sin^2 \theta \cos \theta}$	P	$f_{Ni}$	/F/ calc.	Intensity Calc. $10^5$	Intensity Obs. $10^5$
111	26.12	8.0	8	19	76.0	3.6	3.6
200	30.58	5.5	6	18.2	73.0	1.7	1.8
220	45.90	2.8	12	14.6	58.4	1.1	1.2
311	57.27	3.0	24	13.2	52.8	1.9	1.8
222	61.49	3.5	8	12.7	51.2	0.7	0.7



angle. Hence, no correction for absorption and temperature is necessary.

### Preliminary Investigations

The structure of diamond is shown diagrammatically in Figure 11. The lattice sites are projected on the basal plane and the fractions in circles indicate heights above the basal plane. If this is the structure of  $\text{Ti}_2\text{Ni}$ , the titanium and nickel atoms would be symmetrically arranged around these lattice sites. There are 8 lattice sites per unit cell, therefore to accommodate 96 atoms it is necessary to arrange 12 atoms (8 titanium and 4 nickel) symmetrically around each lattice site. Several arrangements were considered, and coordinates for each arrangement were established. The coordinates showed that the distances between certain pairs of atoms were unreasonably close, thus indicating that the structure of  $\text{Ti}_2\text{Ni}$  could not have the diamond arrangement.

Investigations were then concentrated on the face-centered cubic arrangement. The structure is obtained from a cube comprising of 27 face-centered cubic unit cells. Such a multiple cell contains  $3^3 \times 4 = 108$  lattice points. Each lattice point is now made an atomic site, 12 atoms are removed, and the remaining atoms displaced by small amounts so that the cubic symmetry is preserved.







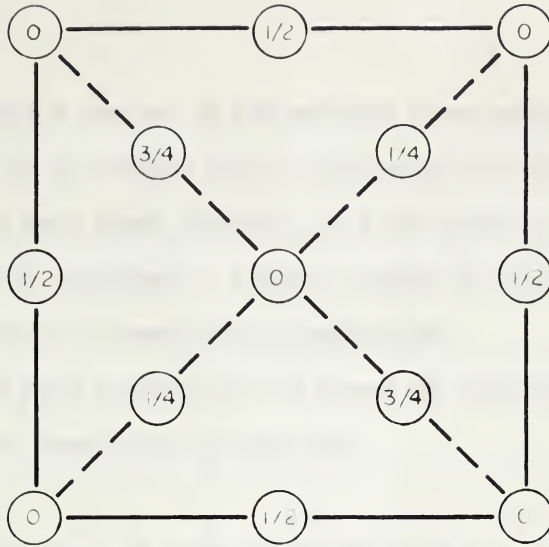


Figure 11. Structure of diamond.

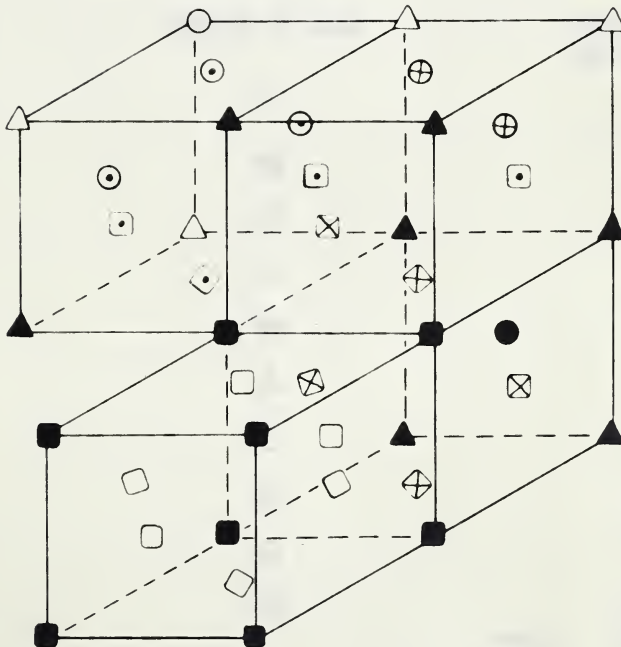


Figure 12. Section of multiple face-centered cubic cell.



Figure 12 shows a section of the multiple face-centered cubic cell. The atoms lie on corners and on face centers of 27 cubes. Since there are so many atoms involved it is not necessary that they be structurally equivalent. However, groups of structurally equivalent atoms must be symmetrically positioned.

The 108 atoms were divided into 10 groups of equivalent positions and type, summarized in Table VII.

Table VII - Arrangement of Atoms in the Multiple Face-centered Cubic Cell.

<u>Type of Atom</u>	<u>Symbol of Type</u>	<u>No. of atoms per unit cell</u>
"A"	○	1
"B"	●	3
"C"	□	6
"D"	△	6
"E"	■	8
"F"	▲	12
"G"	⊙	12
"H"	⊕	12
"I"	◻	24
"J"	⊗	24
TOTAL		<u>108</u>



Table VII shows that there are 5 rational ways in which 12 atoms can be removed. There are, therefore, several possible arrangements which would accommodate 96 atoms in the cell. For each arrangement, each group of atoms may be displaced in a different manner and by a different amount, thus making numerous arrangements possible.

Several arrangements were considered and, intensities were calculated for selected reflections. The calculated intensities were completely incompatible with the observed values. Since there were so many possible arrangements to be considered, it was decided that it might be simpler to obtain the correct arrangement from the  $O_h^7$  space group.

The possible arrangements in the  $O_h^7$  space group of International tables are shown in Table VIII. The 96g and 96h positions were considered first but were rejected since a preliminary examination showed that structures giving line intensities approaching those observed would contain unreasonably small interatomic distances. There remained several possible combinations of 48f, 32e, 16d, 16c, 8b and 8a. In order that the distances between pairs of atoms would be approximately the same as the sum of the atomic radii of the constituent atoms, the most probable coordinates may be shown to be those of 48f, 32e, and 16c. The 32 nickel atoms are most likely to occupy the 32e positions and the 64 titanium atoms to occupy the 48f and 16c positions.





Cubic  $m\bar{3}m$  $Fd_{41/d}\bar{3}2/m$ 

No. 227

 $Fd\bar{3}m$   
 $O_h^7$ Origin at centre ( $\bar{3}m$ ), at  $\frac{1}{4}, \frac{1}{4}, \frac{1}{4}$  from  $\bar{4}3m$  (compare previous page for alternative origin)Number of positions,  
Wyckoff notation,  
and point symmetry

Co-ordinates of equivalent positions

Conditions limiting  
possible reflections(0,0,0;  $0, \frac{1}{4}, \frac{1}{4}$ ;  $\frac{1}{4}, 0, \frac{1}{4}$ ;  $\frac{1}{4}, \frac{1}{4}, 0$ )+

General:

192  $i$  1  $x, y, z$ ;  $x, \frac{1}{4} - y, \frac{1}{4} - z$ ;  $\frac{1}{4} - x, y, \frac{1}{4} - z$ ;  $\frac{1}{4} - x, \frac{1}{4} - y, z$ ;  
 $z, x, y$ ;  $z, \frac{1}{4} - x, \frac{1}{4} - y$ ;  $\frac{1}{4} - z, x, \frac{1}{4} - y$ ;  $\frac{1}{4} - z, \frac{1}{4} - x, y$ ;  
 $y, z, x$ ;  $y, \frac{1}{4} - z, \frac{1}{4} - x$ ;  $\frac{1}{4} - y, z, \frac{1}{4} - x$ ;  $\frac{1}{4} - y, \frac{1}{4} - z, x$ ;  
 $x, z, y$ ;  $x, \frac{1}{4} - z, \frac{1}{4} - y$ ;  $\frac{1}{4} - x, z, \frac{1}{4} - y$ ;  $\frac{1}{4} - x, \frac{1}{4} - z, y$ ;  
 $y, x, z$ ;  $y, \frac{1}{4} - x, \frac{1}{4} - z$ ;  $\frac{1}{4} - y, x, \frac{1}{4} - z$ ;  $\frac{1}{4} - y, \frac{1}{4} - x, z$ ;  
 $z, y, x$ ;  $z, \frac{1}{4} - y, \frac{1}{4} - x$ ;  $\frac{1}{4} - z, y, \frac{1}{4} - x$ ;  $\frac{1}{4} - z, \frac{1}{4} - y, x$ ;  
 $\bar{x}, \bar{y}, \bar{z}$ ;  $\bar{x}, \frac{3}{4} + y, \frac{3}{4} + z$ ;  $\frac{3}{4} + x, \bar{y}, \frac{3}{4} + z$ ;  $\frac{3}{4} + x, \frac{3}{4} + y, \bar{z}$ ;  
 $\bar{z}, \bar{x}, \bar{y}$ ;  $\bar{z}, \frac{3}{4} + x, \frac{3}{4} + y$ ;  $\frac{3}{4} + z, \bar{x}, \frac{3}{4} + y$ ;  $\frac{3}{4} + z, \frac{3}{4} + x, \bar{y}$ ;  
 $\bar{y}, \bar{z}, \bar{x}$ ;  $\bar{y}, \frac{3}{4} + z, \frac{3}{4} + x$ ;  $\frac{3}{4} + y, \bar{z}, \frac{3}{4} + x$ ;  $\frac{3}{4} + y, \frac{3}{4} + z, \bar{x}$ ;  
 $\bar{x}, \bar{z}, \bar{y}$ ;  $\bar{x}, \frac{3}{4} + z, \frac{3}{4} + y$ ;  $\frac{3}{4} + x, \bar{z}, \frac{3}{4} + y$ ;  $\frac{3}{4} + x, \frac{3}{4} + z, \bar{y}$ ;  
 $\bar{y}, \bar{x}, \bar{z}$ ;  $\bar{y}, \frac{3}{4} + x, \frac{3}{4} + z$ ;  $\frac{3}{4} + y, \bar{x}, \frac{3}{4} + z$ ;  $\frac{3}{4} + y, \frac{3}{4} + x, \bar{z}$ ;  
 $\bar{z}, \bar{y}, \bar{x}$ ;  $\bar{z}, \frac{3}{4} + y, \frac{3}{4} + x$ ;  $\frac{3}{4} + z, \bar{y}, \frac{3}{4} + x$ ;  $\frac{3}{4} + z, \frac{3}{4} + y, \bar{x}$ .

 $hkl$ :  $h + k + l, (l + h) = 2n$  $hhl$ :  $(l + h = 2n)$ ;  $\bar{C}$  $0kl$ :  $(k, l = 2n)$ ;  $k + l = 4n$ 

96  $h$  2  $0, x, \bar{x}$ ;  $0, \frac{1}{4} - x, \frac{1}{4} + x$ ;  $\frac{1}{4}, x, \frac{1}{4} + x$ ;  $\frac{1}{4}, \frac{1}{4} - x, \bar{x}$ ;  
 $\bar{x}, 0, x$ ;  $\frac{1}{4} - x, 0, \frac{1}{4} - x$ ;  $\frac{1}{4} + x, \frac{1}{4}, x$ ;  $\bar{x}, \frac{1}{4}, \frac{1}{4} - x$ ;  
 $x, \bar{x}, 0$ ;  $\frac{1}{4} - x, \frac{1}{4} + x, 0$ ;  $x, \frac{1}{4} + x, \frac{1}{4}$ ;  $\frac{1}{4} - x, \bar{x}, \frac{1}{4}$ ;  
 $0, \bar{x}, x$ ;  $0, \frac{3}{4} + x, \frac{3}{4} - x$ ;  $\frac{3}{4}, \bar{x}, \frac{3}{4} - x$ ;  $\frac{3}{4}, \frac{3}{4} + x, x$ ;  
 $x, 0, \bar{x}$ ;  $\frac{3}{4} - x, 0, \frac{3}{4} + x$ ;  $\frac{3}{4} - x, \frac{3}{4}, \bar{x}$ ;  $x, \frac{3}{4}, \frac{3}{4} + x$ ;  
 $\bar{x}, x, 0$ ;  $\frac{3}{4} + x, \frac{3}{4} - x, 0$ ;  $\bar{x}, \frac{3}{4} - x, \frac{3}{4}$ ;  $\frac{3}{4} + x, x, \frac{3}{4}$ .

Special: as above, plus

no extra conditions

96  $g$   $m$   $x, x, z$ ;  $x, \frac{1}{4} - x, \frac{1}{4} - z$ ;  $\frac{1}{4} - x, x, \frac{1}{4} - z$ ;  $\frac{1}{4} - x, \frac{1}{4} - x, z$ ;  
 $z, x, x$ ;  $z, \frac{1}{4} - x, \frac{1}{4} - x$ ;  $\frac{1}{4} - z, x, \frac{1}{4} - x$ ;  $\frac{1}{4} - z, \frac{1}{4} - x, x$ ;  
 $x, z, x$ ;  $x, \frac{1}{4} - z, \frac{1}{4} - x$ ;  $\frac{1}{4} - x, z, \frac{1}{4} - x$ ;  $\frac{1}{4} - x, \frac{1}{4} - z, x$ ;  
 $\bar{x}, \bar{x}, \bar{z}$ ;  $\bar{x}, \frac{3}{4} + x, \frac{3}{4} + z$ ;  $\frac{3}{4} + x, \bar{x}, \frac{3}{4} + z$ ;  $\frac{3}{4} + x, \frac{3}{4} + x, \bar{z}$ ;  
 $\bar{z}, \bar{x}, \bar{x}$ ;  $\bar{z}, \frac{3}{4} + x, \frac{3}{4} + x$ ;  $\frac{3}{4} + z, \bar{x}, \frac{3}{4} + x$ ;  $\frac{3}{4} + z, \frac{3}{4} + x, \bar{x}$ ;  
 $\bar{x}, \bar{z}, \bar{x}$ ;  $\bar{x}, \frac{3}{4} + z, \frac{3}{4} + x$ ;  $\frac{3}{4} + x, \bar{z}, \frac{3}{4} + x$ ;  $\frac{3}{4} + x, \frac{3}{4} + z, \bar{x}$ .

48  $f$   $mm$   $x, \frac{1}{8}, \frac{1}{8}$ ;  $\bar{x}, \frac{7}{8}, \frac{7}{8}$ ;  $\frac{1}{4} - x, \frac{1}{8}, \frac{1}{8}$ ;  $\frac{3}{4} + x, \frac{7}{8}, \frac{7}{8}$ ;  
 $\frac{1}{8}, x, \frac{1}{8}$ ;  $\frac{7}{8}, \bar{x}, \frac{7}{8}$ ;  $\frac{1}{8}, \frac{1}{4} - x, \frac{1}{8}$ ;  $\frac{7}{8}, \frac{3}{4} + x, \frac{7}{8}$ ;  
 $\frac{1}{8}, \frac{1}{8}, x$ ;  $\frac{7}{8}, \frac{7}{8}, \bar{x}$ ;  $\frac{1}{8}, \frac{1}{8}, \frac{1}{4} - x$ ;  $\frac{7}{8}, \frac{7}{8}, \frac{3}{4} + x$ .

 $hkl$ :  $h + k + l = 2n + 1$  or  $4n$ 

32  $e$   $3m$   $x, x, x$ ;  $x, \frac{1}{4} - x, \frac{1}{4} - x$ ;  $\frac{1}{4} - x, x, \frac{1}{4} - x$ ;  $\frac{1}{4} - x, \frac{1}{4} - x, x$ ;  
 $\bar{x}, \bar{x}, \bar{x}$ ;  $\bar{x}, \frac{3}{4} + x, \frac{3}{4} + x$ ;  $\frac{3}{4} + x, \bar{x}, \frac{3}{4} + x$ ;  $\frac{3}{4} + x, \frac{3}{4} + x, \bar{x}$ .

no extra conditions

16  $d$   $\bar{3}m$   $\frac{1}{4}, \frac{1}{4}, \frac{1}{4}$ ;  $\frac{1}{4}, \frac{1}{4}, \frac{1}{4}$ ;  $\frac{1}{4}, \frac{1}{4}, \frac{1}{4}$ ;  $\frac{1}{4}, \frac{1}{4}, \frac{1}{4}$ .

$hkl$ :  $\left. \begin{array}{l} h = 2n + 1 \\ k = 2n + 1 \\ l = 2n + 1 \end{array} \right\}$   
 $\left. \begin{array}{l} 4n + 2 \\ \text{or } 4n + 2 \\ 4n + 2 \end{array} \right\} \begin{array}{l} 4n \\ \text{or } 4n \\ 4n \end{array}$

16  $c$   $\bar{3}m$   $0, 0, 0$ ;  $0, \frac{1}{4}, \frac{1}{4}$ ;  $\frac{1}{4}, 0, \frac{1}{4}$ ;  $\frac{1}{4}, \frac{1}{4}, 0$ .

8  $b$   $\bar{4}3m$   $\frac{1}{4}, \frac{1}{4}, \frac{1}{4}$ ;  $\frac{1}{4}, \frac{1}{4}, \frac{1}{4}$ .

8  $a$   $\bar{4}3m$   $\frac{1}{4}, \frac{1}{4}, \frac{1}{4}$ ;  $\frac{1}{4}, \frac{1}{4}, \frac{1}{4}$ .

 $hkl$ :  $h + k + l = 2n + 1$  or  $4n$





### Calculation of Structure

The parameters for nickel and titanium atoms were determined by trial and error. The intensities of reflections that do not depend on the positions of the 48f titanium atoms depend only on the value of the nickel parameter, since the 16c titanium atoms are invariant. These reflections are 222; 442; 622; 662; 644; 842; and 10,4,4; and 10,6,2. A comparison of the observed and calculated intensities of these reflections gives a best value of  $0.215 \pm .001$  for the parameter of the nickel atoms. For these reflections, the discrepancy factor is 0.19. The change in discrepancy factor with parameter justifies the accuracy quoted. The change in ratio of calculated structure factors for reflections 222 and 442 with the nickel parameter is shown in Figure 13. The observed structure factor ratio for the two reflections is indicated by the horizontal broken line and corresponds to a parameter value of 0.215(5) for nickel. Using the value of 0.215 for nickel atoms, the parameter of the 48f titanium atoms was found by trial and error to be  $0.810 \pm .002$ . Figure 14 shows the change in ratio of the calculated structure factors for reflections 440 and 422 with the titanium parameter. The horizontal broken line represents the observed ratio of the two reflections and corresponds to a parameter value of 0.809(3) for titanium.



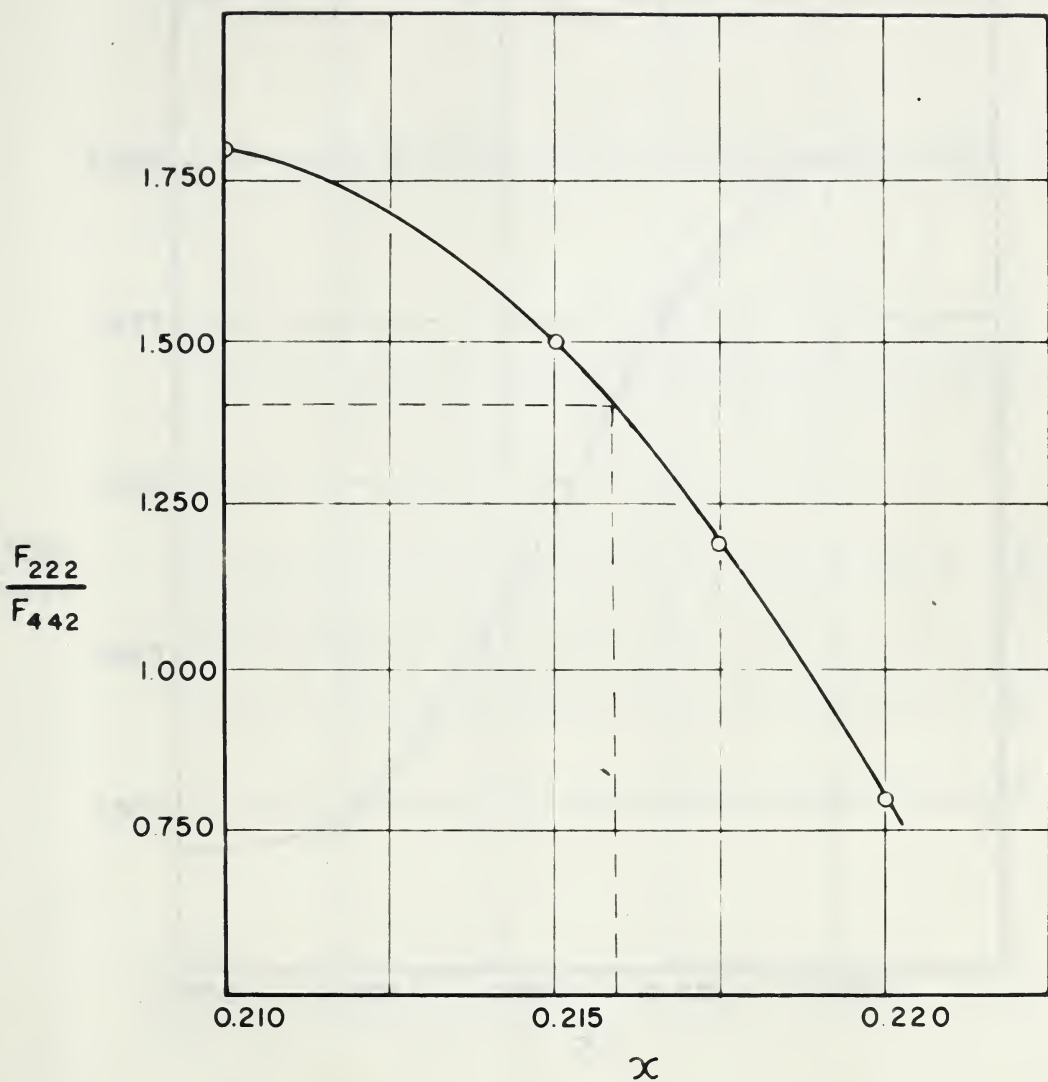


Figure 13. Change in ratio of calculated structure factors with nickel parameter.



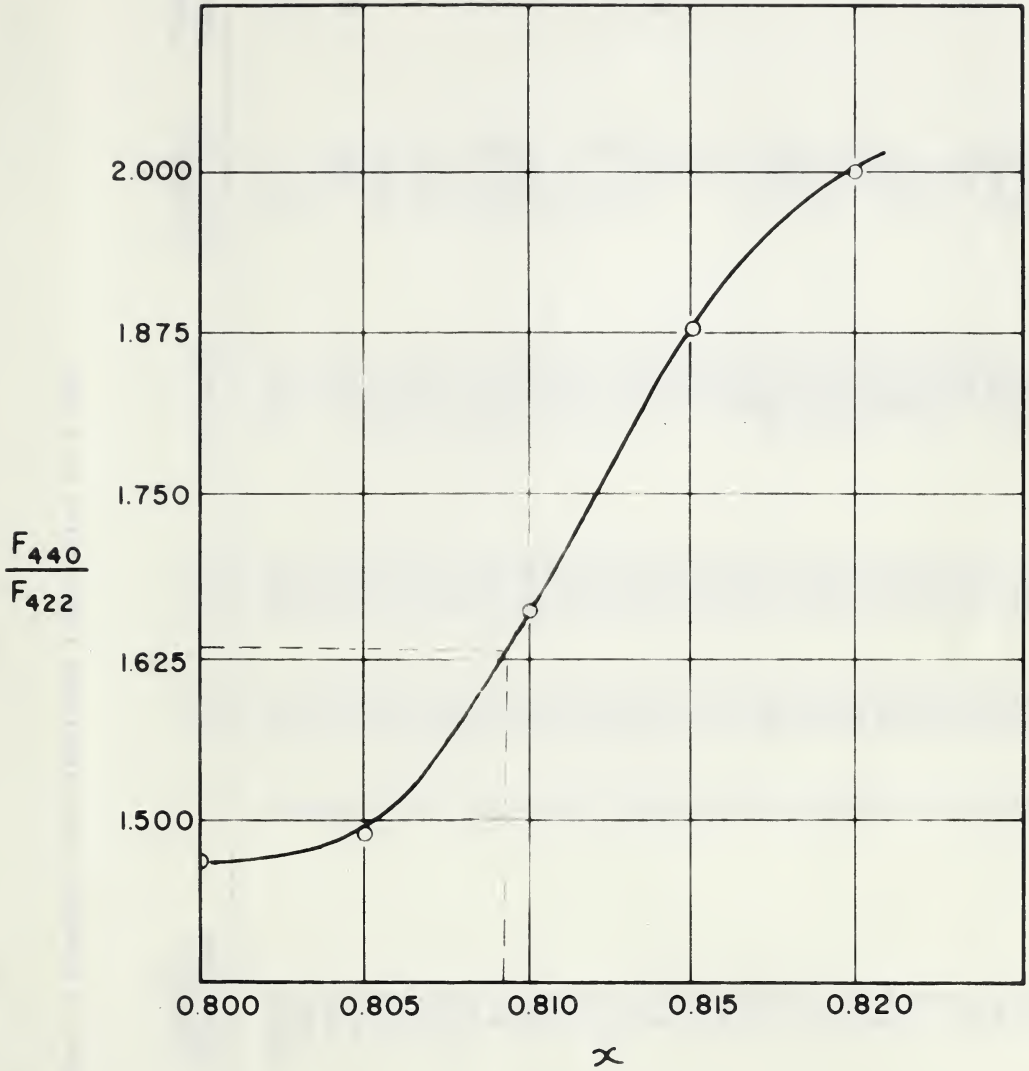


Figure 14. Change in ratio of calculated structure factors with titanium parameter.



Table IX - Comparison of Observed and Calculated Intensities in  $Ti_2Ni$ .

hkl	$\theta$	$\frac{1 + \cos^2 \theta}{\sin^2 \theta \cos \theta}$	P	$f_{Ni}$	$f_{Ti}$	/F/ calc.	Intensity Calc. $10^6$	Intensity Obs. $10^6$
111	7.96	100.3	8	25.7	20.0	-151.3	18.4	16
200	9.00	78.8	6	25.3	19.5	0	0	N.D.
220	12.40	43.4	12	25.0	19.0	-23.1	2.6	2*
311	15.23	24.3	24	23.0	18.0	-12.0	.08	N.D.
222	16.00	23.5	8	22.6	17.8	-251.3	11.8	9
400	18.59	18.5	6	21.6	16.4	194.8	4.2	3*
331	20.24	14.0	24	21.1	16.0	151.2	7.7	6
422	22.89	10.6	24	20.0	15.1	-419.1	44.8	49
511	24.35	9.4	24	19.3	14.6	-729.7	120.2	164
333	24.35	9.4	8	19.3	14.6	775.9	45.3	46
440	26.73	7.5	12	19.0	14.3	695.0	43.5	8
531	27.95	6.8	48	18.1	13.5	178.7	10.4	13
600	28.40	6.7	6	18.1	13.5	0	0	N.D.
442	28.40	6.7	24	18.1	13.5	311.3	15.4	2*
620	30.00	5.8	24	17.7	13.1	-6.2	.06	2*
533	31.30	5.4	24	17.7	13.1	85.5	.9	6'
622	31.59	5.2	24	17.5	12.9	83.4	.9	7
444	33.24	4.5	8	17.0	12.6	380.7	5.2	3*
711	34.46	4.2	24	16.7	12.4	-236.4	5.6	10
551	34.46	4.2	24	16.7	12.4	-135.1	1.8	3*
642	36.82	3.5	48	16.3	12.2	-138.1	3.2	2*
731	37.40	3.5	48	16.3	12.2	-186.3	5.9	N.D.
553	37.40	3.5	24	16.3	12.2	220.9	4.1	44
800	39.30	3.2	6	16.2	12.1	392.4	2.9	14
733	40.36	3.2	24	15.6	11.7	-123.0	1.2	
644	40.77	3.1	24	15.4	11.5	73.3	.4	
822	42.14	3.0	24	15.2	11.4	446.9	14.4	
660	42.14	3.0	12	15.2	11.4	-919.3	30.4	
751	43.28	3.0	48	14.6	10.8	70.5	.7	
555	43.28	3.0	8	14.6	10.8	-703.5	11.9	

\* Estimated value.

N.D. - not detected.







Table IX continued

662	43.55	2.9	24	14.6	10.8	148.2	1.6	2*
840	45.06	2.8	24	14.6	10.8	-56.1	.2	N.D.
911	46.08	2.8	24	14.6	10.8	-226.5	3.4	10
753	46.08	2.8	48	14.6	10.8	175.0	4.2	13
842	46.51	2.8	48	14.6	10.8	320.6	13.8	N.D.
664	48.00	2.7	24	14.4	10.7	-22.4	.03	4
931	48.86	2.7	48	14.4	10.7	133.2	2.3	N.D.
844	51.60	2.8	24	13.3	10.6	-53.1	.02	45
933	52.16	2.8	24	13.0	10.5	636.7	27.2	N.D.
771	52.16	2.8	24	13.0	10.5	135.1	1.2	4
755	52.16	2.8	24	13.0	10.5	-451.5	13.7	N.D.
10,00	52.40	2.8	6	12.9	10.3	0	0	10
862	53.61	2.8	48	12.9	10.3	-130.3	2.3	13
10,20	53.61	2.8	24	12.9	10.3	-291.2	5.7	10
951	54.78	2.9	48	12.8	10.2	-214.3	6.4	10
773	54.78	2.9	24	12.8	10.2	228.6	3.6	9
666	55.76	2.9	8	12.7	10.0	153.9	.6	6
10,22	55.76	2.9	24	12.7	10.0	355.6	8.8	18
775	61.40	3.4	24	12.5	9.7	286.5	6.7	2*
11,11	61.40	3.4	24	12.5	9.7	76.0	.5	12
955	64.70	3.9	24	12.5	9.7	-57.4	.3	35
971	64.70	3.9	48	12.5	9.7	163.7	5.0	47
11,31	64.70	3.9	48	12.5	9.7	-29.0	.2	58
882	65.26	4.0	24	12.4	9.5	170.1	2.8	8
10,44	65.26	4.0	24	12.4	9.5	-346.7	11.5	
866	67.16	4.5	24	12.4	9.5	13.8	.02	
10,60	67.16	4.5	24	12.4	9.5	47.3	.20	
10,62	69.53	5.2	48	12.4	9.5	204.6	10.5	
12,00	71.76	5.6	6	12.3	9.3	618.0	12.8	
884	71.76	5.6	24	12.3	9.3	423.0	24.0	
11,51	73.21	6.3	48	12.2	9.1	-383.8	44.4	
777	73.21	6.3	8	12.2	9.1	36.1	.7	
12,22	77.31	8.5	24	12.2	9.1	-109.8	2.4	
10,64	77.31	8.5	48	12.2	9.1	-383.8	60.0	
11,53	80.08	11.2	48	12.0	9.0	72	2.8	
975	80.08	11.2	48	12.0	9.0	72	2.8	



Table X - Coordinates of Titanium and Nickel Atoms

Titanium atoms

(0 0 0)(0 .25 .25)(.25 0 .25)(.25 .25 0)(0 .50 .50)(.50 0 .50)  
(.50 .50 0)(0 .75 .75)(.75 0 .75)(.75 .75 0)(.25 .50 .75)(.25 .75 .50)  
(.50 .25 .75)(.50 .75 .25)(.75 .25 .50)(.75 .50 .25)  
(.810 .125 .125)(.125 .810 .125)(.125 .125 .810)(.190 .875 .875)  
(.875 .190 .875)(.875 .875 .190)(.440 .125 .125)(.125 .440 .125)  
(.125 .125 .440)(.560 .875 .875)(.875 .560 .875)(.875 .875 .560)  
(.810 .625 .625)(.125 .310 .625)(.125 .625 .310)(.190 .375 .375)  
(.875 .690 .375)(.875 .375 .190)(.440 .625 .625)(.125 .940 .625)  
(.125 .625 .940)(.560 .375 .375)(.875 .060 .375)(.875 .375 .060)  
(.310 .125 .625)(.625 .810 .625)(.625 .125 .310)(.690 .875 .375)  
(.375 .190 .375)(.375 .875 .690)(.940 .125 .625)(.625 .440 .625)  
(.625 .125 .940)(.060 .875 .375)(.375 .560 .375)(.375 .875 .060)  
(.310 .625 .125)(.625 .310 .125)(.625 .625 .810)(.690 .375 .875)  
(.375 .690 .875)(.375 .375 .190)(.940 .625 .125)(.625 .940 .125)  
(.625 .625 .440)(.060 .375 .875)(.375 .060 .875)(.375 .375 .560)

Nickel Atoms

(.215 .215 .215)(.785 .785 .785)(.215 .035 .035)(.035 .215 .035)  
(.035 .035 .215)(.785 .965 .965)(.965 .785 .965)(.965 .965 .785)  
(.215 .715 .715)(.785 .285 .285)(.215 .535 .535)(.035 .715 .535)  
(.035 .535 .715)(.785 .465 .465)(.965 .285 .465)(.965 .465 .285)  
(.715 .215 .715)(.285 .785 .285)(.715 .035 .535)(.535 .215 .535)  
(.535 .035 .715)(.285 .965 .465)(.465 .785 .465)(.465 .965 .285)  
(.715 .715 .215)(.285 .285 .785)(.715 .535 .035)(.535 .715 .035)  
(.535 .535 .215)(.285 .465 .965)(.465 .285 .965)(.465 .465 .785)



The comparison of observed and calculated intensities is recorded in Table IX. The discrepancy factor for all 43 reflections is 0.10. The coordinates of the titanium and nickel atoms are shown in Table X.

The calculated intensities for the reflections  $h00 \neq 4n$  are zero. This condition is not specified in the  $O_h^7$  space group. Whether this condition satisfies all the arrangements in this space group, requires further investigation.

#### DISCUSSION OF STRUCTURE

A model of the structure cell is shown in Figure 15. (While the calculation has the center of cell as origin, the model shows a displacement of  $\frac{1}{2} \frac{1}{2} \frac{1}{2}$  so that the atoms are located at cell corners.) In the cell, as in the parent metals, the coordination number of all atoms is 12. The nickel atoms (32e) form regular tetrahedra and the titanium atoms (48f) form regular octahedra. This is indicated in Figure 16 which shows a representative portion of the cell. Each nickel atom has 3 nickel atoms and 9 titanium atoms as nearest neighbors, while the titanium atoms have either 2 nickel and 10 titanium, 4 nickel and 8 titanium, or 6 nickel and 6 titanium atoms as nearest neighbors. These results, together with the interatomic distances, are summarized in Table XI.





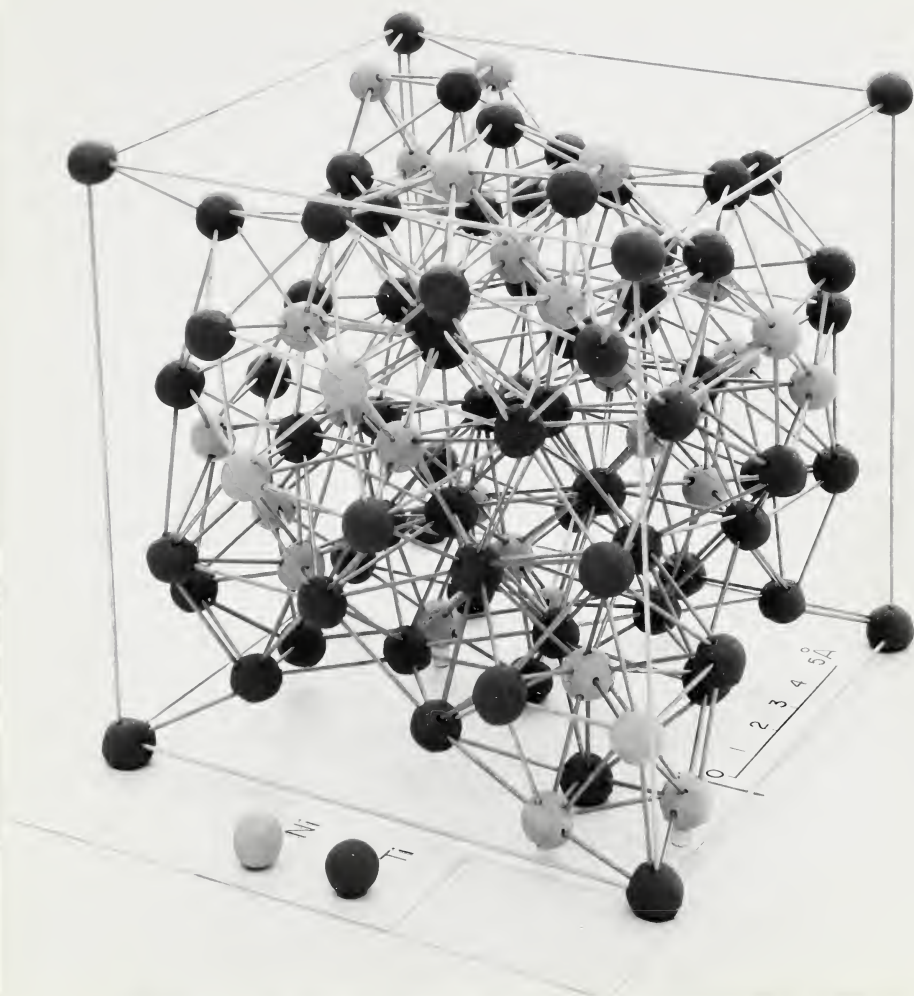


Figure 15. Model of  $\text{Ti}_2\text{Ni}$  structure cell.





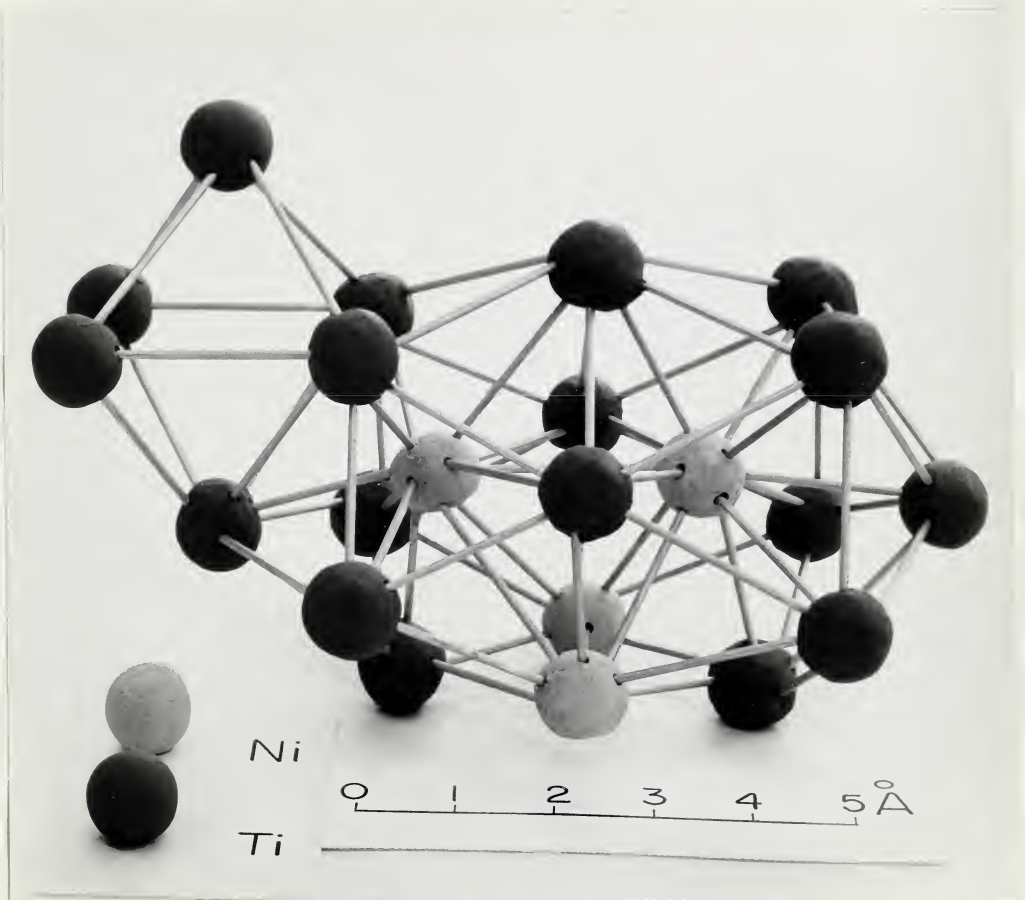


Figure 16. Representative portion of cell.



The titanium atoms are approximately the same distance apart as in pure titanium ( $2.93 \text{ \AA}$ ), while the distance between nickel atoms is greater than that in pure nickel ( $2.49 \text{ \AA}$ ). On the basis of atomic radii, one would expect the Ti - Ni distance to be  $2.71 \text{ \AA}$  whereas the actual distances are  $2.4(9)$ ,  $2.5(7)$  and  $2.9(1) \text{ \AA}$ , with an average length of  $2.66 \text{ \AA}$ , since there are equal numbers of each type. This indicates an increased tendency towards covalency between titanium and nickel atoms. That is, stronger bonding between titanium and nickel atoms. This type of bonding is discussed by Pauling<sup>12</sup>, Hume-Rothery and Coles<sup>13</sup> and Kiessling<sup>14</sup> making particular references to the transition metals. The strength of the Ti - Ni bond is consistent with the large Ni - Ni distance, since each group of 4 Ni atoms is completely surrounded by Ti atoms.

It must be remembered that the assumption that atoms are spherical is a convenient aid rather than a realized fact. Assuming that all atoms are in contact with each other, approximate average diameters of titanium and nickel atoms may be evaluated from interatomic distances. The average nickel diameter ( $2.71 \text{ \AA}$ ) is larger than that for pure nickel ( $2.49 \text{ \AA}$ ) while the average titanium diameter ( $2.82 \text{ \AA}$ ) is smaller than that for pure titanium ( $2.93 \text{ \AA}$ ). Although the calculations are approximate, they do indicate that the size of the nickel atoms has increased at the



Table XI - Interatomic Distances in  $\text{Ti}_2\text{Ni}$ .

<u>Atom</u>	<u>Type of Bond</u>	<u>No. of Bonds</u>	<u>Distance (<math>\text{\AA}</math>)</u>
Ni	Ni - Ni	3	$2.87 \pm .04$
	Ni - Ti	3	$2.49 \pm .02$
	Ni - Ti	3	$2.57 \pm .05$
	Ni - Ti	3	$2.91 \pm .05$
		<u>12</u>	
Ti	Ti - Ni	2	$2.57 \pm .05$
	Ti - Ti	2	$2.93 \pm .02$
	Ti - Ti	8	$2.95 \pm .05$
		<u>12</u>	
Ti	Ti - Ni	2	$2.57 \pm .05$
	Ti - Ni	2	$2.91 \pm .05$
	Ti - Ti	2	$2.93 \pm .02$
	Ti - Ti	6	$2.95 \pm .05$
		<u>12</u>	
Ti	Ti - Ni	6	$2.49 \pm .02$
	Ti - Ti	6	$2.93 \pm .00$
		<u>12</u>	



expense of the titanium atoms. Electron transfer, (postulated in transition metals<sup>14</sup>) from titanium to nickel is probably associated with the increase in size of the nickel atom and the decrease in the size of the titanium atom.





## SUMMARY OF RESULTS AND CONCLUSIONS

1. X-ray diffraction results show that the lattice parameter of  $\text{Ti}_2\text{Ni}$  is the same on both sides of stoichiometric composition. Therefore, if Vegard's law is assumed, a range of composition of not more than 2 pct is indicated.
2. Microscopical metallography shows that single-phase structures are produced by quenching from  $700^\circ\text{C}$  alloys containing 0.5 pct Ni more than or less than stoichiometric composition. Alloys containing 1 pct Ni more than or less than stoichiometric composition show two-phase structures. It is therefore concluded that at  $700^\circ\text{C}$  the composition limits for  $\text{Ti}_2\text{Ni}$  lie between 0.5 and 1 pct Ni on either side of the stoichiometric composition.
3. Alloys containing 0.5 pct more than or less than stoichiometric composition when quenched from  $900^\circ\text{C}$  or slow cooled from  $700^\circ\text{C}$  show two-phase structures. It is therefore concluded that the composition limits decrease above  $900^\circ\text{C}$  and below  $700^\circ\text{C}$ .
4. The maximum limits of composition for  $\text{Ti}_2\text{Ni}$  lie between  $700^\circ$  and  $900^\circ\text{C}$ ; at  $765^\circ\text{C}$  on the minimum nickel content side and between  $800^\circ$  and  $900^\circ\text{C}$  on the maximum nickel content side.



5. The structure of  $\text{Ti}_2\text{Ni}$  is face-centered cubic with a cell parameter of  $11.278 \pm .001 \text{ \AA}$  and density of  $5.723 \pm .001 \text{ g. cm}^{-3}$  from which the number of atoms per unit is calculated as 96.0.

6. The space group is  $O_h^7$  -  $\text{Fd}3\text{m}$ . 64 titanium atoms are in positions 48f and 16c, and 32 nickel atoms are in positions 32e. The atomic parameters,  $X_{\text{Ni}} = 0.215 \pm .001$  and  $X_{\text{Ti}} = 0.810 \pm .002$ , were determined by trial and error.

7. The interatomic distances were calculated and discussed. The Ni - Ni distance is  $2.87 \text{ \AA}$ , while the Ti - Ni distances are 2.49, 2.57 and  $2.91 \text{ \AA}$  and the Ti - Ti distances are 2.93 and  $2.95 \text{ \AA}$ .



BIBLIOGRAPHY

1. Laves, F. and Wallbaum, H.J. Naturwissenschaften, Vol.27, (1939), p. 674.
2. Wallbau, H.J. Naturwissenschaften, Vol.14, (1940-41), p. 521.
3. Long, J.R. Metal Progress, Vol.55, (1949), p. 364.
4. McQuillan, A.D. Journal Inst. of Metals, Vol.18, (1950), p.249.
5. Margolin, H., Ence, E. and Nielsen, J.P. Trans. A.I.M.E., Vol.197, (1953), p. 243;  
Journal of Metals, Feb. 1953, Supplement.
6. Duwez, F. and Taylor, J.L. Trans. A.I.M.E., Vol.188, (1950), p. 1173.
7. Hansen, M., McPherson, D.J. and Rostoker, W. W.A.D.C. Tech. Rep. No. 53-41, (1953).
8. Rostoker, W. Journal of Metals, Vol.4, (1952), p. 209.
9. International Tables for X-ray Crystallography, Vol.1, (1952).
10. Taylor, A. An Introduction to X-ray Metallography, Table XXXV, Appendix.
11. Lipson, H. and Cochran, W. The Determination of Crystal Structures, Vol.3, Appendix VII, p. 323.
12. Pauling, L. Journal of Amer. Chem. Soc. Vol.69, (1947), p. 542.
13. Hume-Rothery, W. and Coles, B.R. Advances in Physics, Vol.3, (1954), p. 149.
14. Kiessling, R. Metallurgical Reviews, Vol.1-2, (1956-57), p.77.





## APPENDICES



## APPENDIX I

### LEVITATION MELTING

Titanium has a high affinity for  $O_2$ ,  $N_2$  and  $H_2$  at elevated temperatures. Therefore, it is necessary to prepare titanium alloys in either a vacuum or an inert atmosphere. Titanium is also reactive with all refractory oxides and with carbon at temperatures over  $700^{\circ}C$ . Consequently, it may not come into contact with refractory materials both during heat treatment and melting.

Arc melting and levitation melting are two methods available for preparing titanium alloys. Levitation melting<sup>1</sup> is advantageous over arc melting since it produces homogeneous alloys on first casting.

The levitation unit is shown in Figure 1. The conical induction coil contains 5 parallel turns and an additional upper reversed turn. The upper reversed turn stabilizes the electromagnetic field in the coil. The melt is poured through the lower turn into a copper mold, by reducing the current to the coil. The coil was made from 1/8" diameter bright annealed copper tubing and is energized by a 12 kw. 1300 kc. source available from a Philips High Frequency Generator. The unit is enclosed in a lucite cylinder and brass end plates.



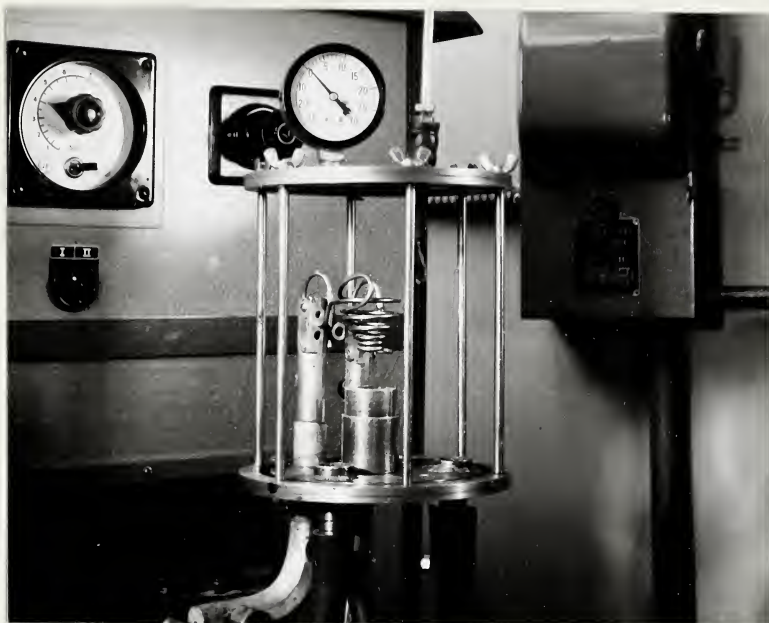


Figure 1. Levitation melting unit.

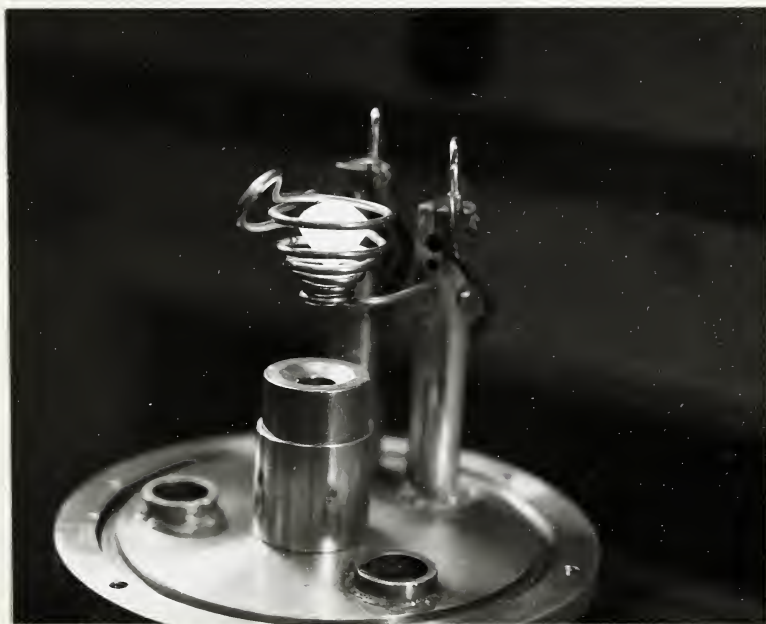


Figure 2. Levitation melting unit in operation.



Figure 2 shows the levitation unit in operation. Levitation and casting were carried out in a high purity argon atmosphere under a positive pressure of 10" of mercury.

Reference:

- (1) Polonis, D. H., Butters, R. G., and Parr, J. G.  
Research 7, 510, (1954), p. 272.





## APPENDIX II

### GAS QUENCHING

All possible precautions against contamination were necessary for the present investigations, especially since powder specimens were used — which made more surface area available to contamination. Even minute traces of oxygen and nitrogen in an inert atmosphere will cause sufficient contamination to affect the results of investigations. Therefore, the argon that was used for an inert atmosphere was purified by passing it through a purification furnace containing sponge titanium (to remove oxygen and nitrogen) and  $P_2O_5$  (to remove water vapour).

The furnace used for quenching Ti-Ni powder specimens with argon ( $-60^{\circ}\text{C}$ ) was designed by Swann and Parr<sup>1</sup> in 1957 and is shown in Figure 1.

The important features of this furnace are: (1) A positive pressure of purified argon is maintained in the furnace at all times — even when the specimen is removed or inserted. (2) The furnace tube is Inconel — a nickel-chromium alloy which is corrosion resistant at high temperatures. Inconel will not react with the molybdenum boat, thus assuring free movement of the boat along the tube.

The specimen is introduced in the quenching furnace in the



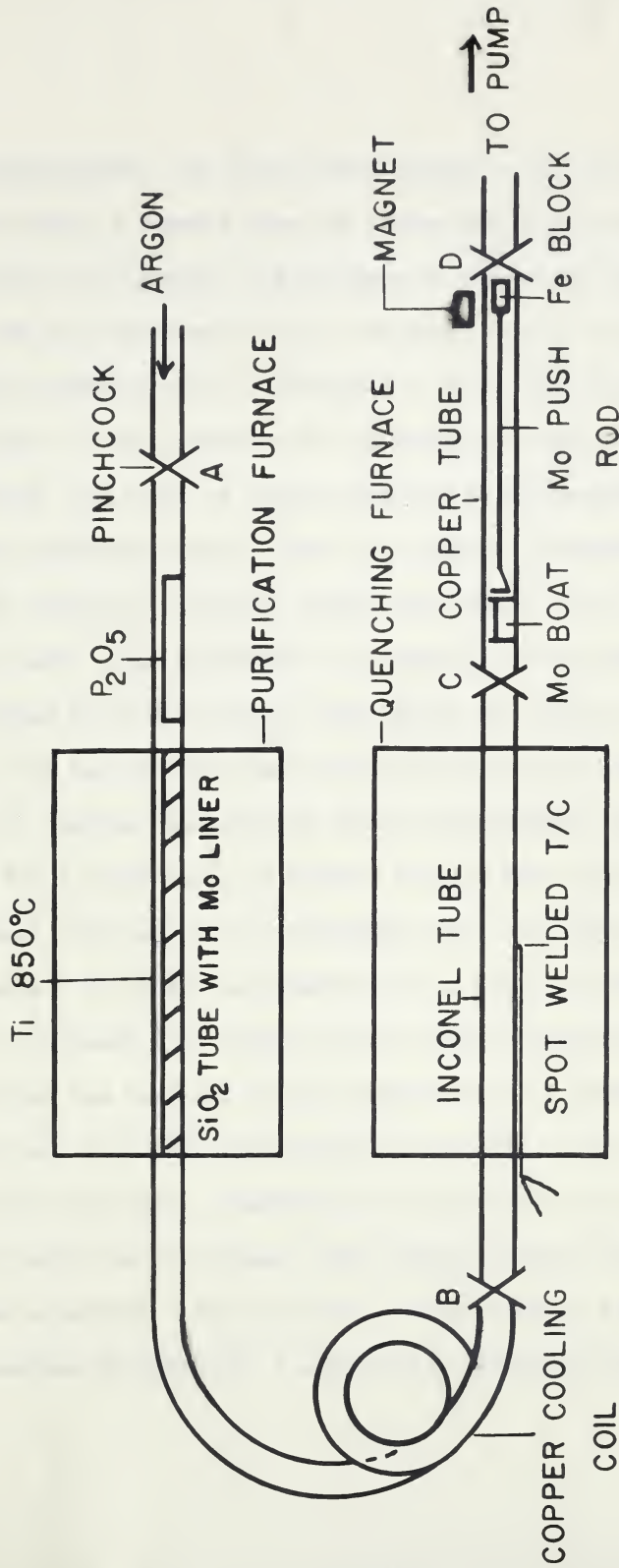


Figure 1. Gas quenching unit for powder specimens.



following manner: The glass tube (placed at the end of the copper tube) is removed from the vacuum end of the furnace after pinchcock C is closed. The specimen is placed in front of the push rod in a molybdenum boat. The glass tube is replaced and is then evacuated back to pinchcock C to  $10^{-4}$  mm of mercury, and maintained at that pressure for 10 minutes. Next, pinchcock D is closed, and argon is slowly admitted to the evacuated tube through pinchcock C until there is a positive pressure inside it. This is repeated 3 times to insure that there is no trace of air in the tube. Then pinchcock C is removed and the glass tube is positioned up to the Inconel tube inside the rubber connecting tube. The specimen is then slid into the furnace with a magnet until it reaches the position of the thermocouple, and is left there for 15 minutes. (15 minutes insures that equilibrium is reached.) The push rod is withdrawn using the magnet again. Pinchcock B is closed and pinchcock D is opened to evacuate the tube. Pinchcock B is opened and the rush of argon through the tube blows the boat out of the furnace until it reaches the front of the push rod, and the specimen is quenched by the rush of pure argon into the pump. Pinchcock D is closed and the glass tube is pulled away from the Inconel tube leaving enough "free" rubber so that pinchcock C may be closed. After closing pinchcock C, the specimen is removed. A screen trap placed at the end of the





copper tube was used as a safety precaution so that if the powder was blown out of the boat, it would be caught in the trap. This trap not only saved the specimen but it also prevented damage to the pump.

Reference:

- (1) P. R. Swann and J. G. Parr, Trans. A.I.M.E. Vol. 212,  
April 1958, pp. 276-279.









**B29781**